DYNAMIC MODELS OF SERVO-DRIVEN CONVEYOR SYSTEM

Jitkomut Songsiri   David Banjerdpongchai

Department of Electrical Engineering, Chulalongkorn University
254 Phayathai Road, Pathumwan, Bangkok, 10330, Thailand.
Tel: (+662) 218-6487, Fax: (+662) 251-8991, Email: bdavid@chula.ac.th

ABSTRACT

This paper concerns dynamics of a servo-driven conveyor system, which has been developed for the laboratory-scale experiments. This system consists of a belt lying on the iron plate with two shafts at the end. A DC motor is used to drive the belt through the shaft. The belt is considered to behave like a nonlinear spring. We include the Lugre friction in this model. Then, the dynamics of the conveyor system are derived based on certain specified assumptions. At the same time, the linear and linearized model is used to analyze the behaviors for small signals. Finally, the time responses of these models are shown to verify the modelling analysis

1. INTRODUCTION

Nowadays, one of widely used transportations systems in industries is the conveyor system. In control engineering, understanding its physical model and control problems are the first important issues to design a suitable controller in real condition. Therefore, in this work, we study the models of this system with consideration of the real application.

There are many researches involving the modelling of this system. For example, the dynamical equations of a double conveyor system were derived in [1]. They considered the belt displacement as a simple linear proportion to the motor angle. More complicated model was described in [2]. The belt was first divided into N sections and each of them was modelled as a spring-mass-damper system. All spring-damper parameters were assumed to be constants. On the contrary, the parameters were assumed to be a known function of the mass in [3]. Thus, the results are the nonlinear model.

In this work, we model the belt as the spring-mass system. However, we additionally include the nonlinearity of spring and the so-called Lugre friction model which considers the internal dynamic of the friction.

This paper is organized as follows. We first review the principle and how to model the nonlinear spring and the friction in section 2. Then, modelling of the conveyor system will be described in section 3-5. It includes the dynamical equations, the linear model which is neglected all nonlinearities, and the linearized model obtained from the linearization at the equilibrium points. Section 6 shows the simulation results of all models, and finally, conclusions will be discussed in section 7.

2. SPRING AND FRICTION IN MOTION DYNAMICS

In this section, the mathematical models of spring and friction are considered. These two mechanical elements are the practical nonlinearities which will be included in the model of the servo-driven conveyor. The dynamics of the nonlinear spring and the friction are described in this section.

2.1. Nonlinear Spring

According to [4], there is a description of two kinds of the nonlinear spring. The simplest model of nonlinear (or cubic) spring force can be described by

$$F_s(x) = -kx - bx^3 \tag{1}$$

where k, b are spring parameters.

The sign of b has an effect on spring characteristic. In particular, if $b < 0$ (soft spring), the maximum displacement increases and the maximum acceleration decreases. If $b > 0$ (hard spring), the spring has a smaller displacement and a greater acceleration than a linear spring.

2.2. Friction

The well-known friction models like the viscous plus coulomb memoryless model or the Armstrong model are the static functions of the velocity. In real systems, the friction does not have an instantaneous response when the velocity changes. This is because, in fact, the friction has its own internal dynamics which is proposed by Lugre [5, 6]. For this reason, this model is chosen to represent the friction in this work.

Let p be a state variable of the friction dynamic. It can be described by the following differential equation.

$$\frac{dp}{dt} = \dot{x} - \frac{|v|}{g(\dot{x})}p. \tag{2}$$

where $\dot{x}$ is the relative velocity between two contacted surfaces and g is a monotonically decreasing positive function which describes the Stribeck effect to capture the motion behavior at low velocity.

$$\sigma_0 g(\dot{x}) = F_c + (F_s - F_c)e^{-(\dot{x}/v_s)^2} \tag{3}$$

where F_c, F_s, and v_s are coulomb parameter, stiction parameter, and Stribeck velocity respectively.

The frictional force is described by

$$F_f(\dot{x}) = \sigma_0 p + \sigma_1 \frac{dp}{dt} + F_v\dot{x} \tag{4}$$

where σ_0, σ_1, F_v are stiffness, damping coefficient, and viscous parameter, respectively.

Next section, we will use the knowledge of these nonlinearities to characterise the behavior of the conveyor belt.

3. NONLINEAR DYNAMIC MODEL

Consider the conveyor system depicted in Fig. 1, which consists of the belt lying on the iron plate with two

0-7803-8560-8/04/$20.00©2004IEEE

Fig. 1. Physical system

shafts at the end. A DC motor is used to drive the belt through the shaft to transfer a load mass to the desired position. In this work, we model the belt by dividing it into N sections as shown in Fig. 2. Each section is modeled as a spring-mass system which includes the nonlinear characteristic of the spring. τ is the motor torque and θ is the motor angle. x_j, x_m is the displacement of the j^{th} section and the load mass, respectively. The system parameters are described in Table 1 which

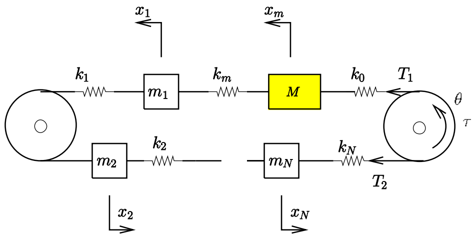

Fig. 2. N-section model of the belt

the motor parameter value are adapted from [7] and the friction parameter value are chosen by the guideline in [5]. Consider the free-body diagram in Fig. 2, we can apply the Newton's law and write the dynamics of each section as follows.

$$M\ddot{x}_m = -F_f^m + F_s^m(x_1 - x_m) - F_s^0(x_m - r\theta) \quad (5)$$

$$m_j\ddot{x}_j = -F_f^j + F_s^j(x_{j-1} - x_j) - F_s^{j+1}(x_j - x_{j+1}) \quad (6)$$

$$m_N\ddot{x}_N = -F_f^N + F_s^N(r\theta - x_N) - F_s^{N-1}(x_N - x_{N-1}) \quad (7)$$

where j is an integer in $[0, N-1]$ indicating the j^{th} section of the belt. F_f^a is the friction force described in (4) and F_s^a is the spring force according to (1) with the notation

$$F_s^a(y_1 - y_2) = k_a(y_1 - y_2) + b_a(y_1 - y_2)^3$$

The superscript a on F_f's and F_s's refers to the force acting on the j^{th} belt section if $a = j$, and on the load mass element if $a = m$.

Next, consider the motor dynamics

$$J\ddot{\theta} = \tau + r(T_1 - T_2) \quad (8)$$

where T_1 and T_2 are the tension shown in Fig. 2 and described by

$$T_1 = k_0(x_m - r\theta)\ , \quad T_2 = k_N(r\theta - x_N) \quad (9)$$

Substituting (9) into (8), we get

$$\ddot{\theta} = \frac{\tau}{J} + \frac{rk_0x_m}{J} + \frac{rk_Nx_N}{J} - \frac{r^2\theta}{J}(k_0 + k_N) \quad (10)$$

The relationship between the motor torque, τ and the armature current, i_a is

$$\tau = K_m i_a \quad (11)$$

The armature current satisfies the dynamic of electrical circuit.

$$\dot{i}_a = \frac{V}{L} - \frac{R}{L}i_a - \frac{K_b\dot{\theta}}{L} \quad (12)$$

where V is the voltage supplied to the motor.

Substitute (11) into (10), we get

$$\ddot{\theta} = \frac{K_m}{J}i_a + \frac{rk_0x_m}{J} + \frac{rk_Nx_N}{J} - \frac{r^2\theta}{J}(k_0 + k_N) \quad (13)$$

In summary, the dynamical equations of this system are described by (5)-(7), (12), and (13).

Table 1. Parameters of the servo-driven conveyor system.

Parameter	Notation	Value	Unit
Load Mass	M	0.5	Kg
Belt mass of the i^{th} section	m_i	0.01	Kg
Spring constant 1	k_i	20	N/m
Spring constant 2	b_i	20	N/m^3
Hub inertia	J	0.01	Kg $\cdot$m^2
Torque constant	K_m	2	N.m/A
Back emf. constant	K_b	0.1	Volt/rad
Resistance	R	1	Ω
Inductance	L	0.5	H
Motor radius	r	0.1	m
Stiffness	σ_0	10	N/m
Damping	σ_1	$\sqrt{10}$	Ns/m
Coulomb friction of the i^{th} section	F_c^i	$1 \times m_i$	N
Viscous friction	F_v	0.5	N
Stiction friction of the i^{th} section	F_s^i	$2 \times F_c$	N
Stribeck velocity	v_s	0.001	m/s

4. LINEARIZED DYNAMIC MODEL

In this section, we include the effect of friction by using the Lugre model and also consider the effect of nonlinear spring characteristic.

For $N = 1$, the dynamical equations (4), (5)-(7), (12), and (13) can be rewritten into the general form, $\dot{z} = f(z, u)$ where z and u are defined as

$$z = [x_m \;\; x_1 \;\; \dot{x}_m \;\; \dot{x}_1 \;\; \theta \;\; \dot{\theta} \;\; I \;\; p_m \;\; p_1]^T\ , \quad u = V.$$

$$\begin{aligned}
f_1 &= z_3 \quad , \quad f_2 = z_4 \\
f_3 &= \frac{1}{M}\Big\{-\sigma_0 z_8 + \frac{\sigma_1|z_3|z_8}{g(z_3)} - (\sigma_1 + F_v)z_3 + k_m(z_2 - z_1) \\
&\quad + b_m(z_2 - z_1)^3 - k_0(z_1 - rz_5) - b_0(z_1 - rz_5)^3\Big\} \\
f_4 &= \frac{1}{m_1}\Big\{-\sigma_0 z_9 + \frac{\sigma_1|z_4|z_9}{g(z_4)} - (\sigma_1 + F_v)z_4 + k_1(rz_5 - z_2) \\
&\quad + b_1(rz_5 - z_2)^3 - k_m(z_2 - z_1) - b_m(z_2 - z_1)^3\Big\} \\
f_5 &= z_6 \qquad\qquad\qquad\qquad\qquad\qquad\qquad\qquad\qquad (14) \\
f_6 &= \frac{1}{J}\left\{K_m z_7 + rk_0 z_1 + rk_1 z_2 - r^2(k_0 + k_1)z_5\right\} \\
f_7 &= \frac{1}{L}\left\{-Rz_7 - K_b z_6 + u\right\} \\
f_8 &= z_3 - \frac{|z_3|}{g(z_3)}z_8 \quad , \quad f_9 = z_4 - \frac{|z_4|}{g(z_4)}z_9
\end{aligned}$$

The equilibrium points can be solved from (14) as follows.

$$z^* = [\alpha \;\; \alpha \;\; 0 \;\; 0 \;\; \alpha/r \;\; 0 \;\; 0 \;\; 0 \;\; 0]^T \quad (15)$$

where α is an arbitrary constant.

To find the linearized model, we need to calculate the Jacobian matrix of $f(z,u)$. However, since there is an absolute operator appear in the system equation, that term is not absolutely differentiable at the equilibrium point. According to [8], we can use the *generalized derivative* of f at z^* as,

$$\tilde{J} = (1-q)J_- + qJ_+ \ , \qquad 0 \le q \le 1$$

where J_- and J_+ are, respectively, the left and right Jacobian matrices, which are calculated from

$$J_- = \begin{bmatrix} \frac{\partial f_1^-}{\partial z} & \frac{\partial f_2^-}{\partial z} & \cdots & \frac{\partial f_n^-}{\partial z} \end{bmatrix}^T$$

$$J_+ = \begin{bmatrix} \frac{\partial f_1^+}{\partial z} & \frac{\partial f_2^+}{\partial z} & \cdots & \frac{\partial f_n^+}{\partial z} \end{bmatrix}^T$$

$$\frac{\partial f_i^-}{\partial z_i} = \lim_{z_i \uparrow 0} \frac{f(z_i,h) - f(0,z_i)}{z_i}$$

$$\frac{\partial f_i^+}{\partial z_i} = \lim_{z_i \downarrow 0} \frac{f(z_i,h) - f(0,z_i)}{z_i}$$

Since the left and right Jacobian at the equilibrium point of this system are equal, the dynamic model around the equilibrium points becomes

$$\dot{z} = \tilde{J}(z^*)z + \left.\frac{\partial f}{\partial u}\right|_{z^*} u \qquad (16)$$

or, in other words,

$$\begin{aligned}
\dot{z}_1 &= z_3 \quad , \quad \dot{z}_2 = z_4 \\
\dot{z}_3 &= \frac{1}{M}\{(k_0+k_m)z_1 + k_m z_2 - (\sigma_1 + F_v)z_3 + \\
&\quad rk_0 z_5 - \sigma_0 z_8\} \\
\dot{z}_4 &= \frac{1}{m_1}\{k_m z_1 - (k_1+k_m)z_2 - (\sigma_1 + F_v)z_4 + \\
&\quad rk_1 z_6 - \sigma_0 z_9\} \\
\dot{z}_5 &= z_6 \qquad\qquad\qquad\qquad\qquad\qquad\qquad (17) \\
\dot{z}_6 &= \frac{1}{J}\{rk_0 z_1 + rk_1 z_2 - r^2(k_0+k_1)z_5 + K_m z_7\} \\
\dot{z}_7 &= \frac{1}{L}\{-K_b z_6 - Rz_7 + u\} \ , \ \dot{z}_8 = z_3 \ , \ \dot{z}_9 = z_4
\end{aligned}$$

Using the assumed parameters shown in Table 1, the eigenvalues of the linearized model (17) are -352.03, -11.8311, $-1.76 \pm 9.73j$, $-3.86 \pm 6.68j$, -0.46, 0, and 0. Two integrators are the results from adding the internal state of friction model

5. LINEAR DYNAMIC MODEL

When neglecting the nonlinearity of spring and friction, we obtain linear dynamical equations as follows,

$$\ddot{x}_m = \frac{k_0}{M}r\theta - \frac{k_0+k_m}{M}x_m + \frac{k_m}{M}x_1 \qquad (18)$$

$$\ddot{x}_1 = \frac{k_m}{m_1}x_m - \frac{k_m+k_1}{m_1}x_1 + \frac{k_1}{m_1}x_2 \qquad (19)$$

$$\ddot{x}_2 = \frac{k_1}{m_2}x_1 - \frac{k_1+k_2}{m_2}x_2 + \frac{k_2}{m_2}x_3 \qquad (20)$$

$$\ddot{x}_i = \frac{k_{i-1}}{m_i}x_{i-1} - \frac{k_{i-1}+k_i}{m_i}x_i + \frac{k_i}{m_i}x_{i+1} \qquad (21)$$

$$\ddot{x}_N = \frac{k_{N-1}}{m_N}x_{N-1} - \frac{k_{N-1}+k_N}{m_N}x_N + \frac{k_N}{m_N}r\theta \qquad (22)$$

$$\ddot{\theta} = \frac{K_m}{J}i_a + \frac{rk_0x_m}{J} + \frac{rk_Nx_N}{J} - \frac{r^2\theta}{J}(k_0+k_N) \qquad (23)$$

$$\dot{i}_a = \frac{V}{L} - \frac{R}{L}i_a - \frac{K_b}{L}\dot{\theta} \qquad (24)$$

Define z, u, y to be state variable, input, and output of the model, respectively.

$$z = [x_m \ x_1 \ \ldots \ x_N \ \dot{x}_m \ \dot{x}_1 \ \ldots \ \dot{x}_N \ \theta \ \dot{\theta} \ I]^T$$

$$u = V, \qquad y = [x_m \ \theta]^T$$

We can rearrange (18)-(24) into the state-space form,

$$\dot{z} = Az + Bu \ , \quad y = Cz.$$

For example, in case $N = 1$ and the parameters given in Table 1, we get the system matrices A, B, C, D as follows.

$$A = \begin{bmatrix} 0 & 0 & 1 & 0 & 0 & 0 & 0 \\ 0 & 0 & 0 & 1 & 0 & 0 & 0 \\ -80 & 40 & 0 & 0 & 4 & 0 & 0 \\ 2000 & -4000 & 0 & 0 & 200 & 0 & 0 \\ 0 & 0 & 0 & 0 & 0 & 1 & 0 \\ 200 & 200 & 0 & 0 & -40 & 0 & 200 \\ 0 & 0 & 0 & 0 & 0 & -0.2 & -2 \end{bmatrix} \quad B = \begin{bmatrix} 0 \\ 0 \\ 0 \\ 0 \\ 0 \\ 0 \\ 2 \end{bmatrix}$$

$$C = \begin{bmatrix} 1 & 0 & 0 & 0 & 0 & 0 & 0 \\ 0 & 0 & 0 & 0 & 1 & 0 & 0 \end{bmatrix} \qquad (25)$$

The eigenvalues of the linear model are $\pm 63.48j$, $-0.2006 \pm 10.34j$, $-0.800 \pm 4.65j$, and 0.

It is noted that an integrator of this model is not ralated to one of two integrators in the linearized model, but is the result from the motor characteristic. This pole is shifted slightly to be -0.46 in the linearized model. When comparing the remaining six complex eigenvalues, $\pm 63.48j$ correspond to $-352.03, -11.8311$ in linearized model. Similarly, $-0.2006 \pm 10.34j$ match $-1.76 \pm 9.73j$ and $-0.800 \pm 4.65j$ correspond to $-3.86 \pm 6.68j$. In brief, the complex eigenvalues of the linear model are shifed to those which are damper in the linearized model due to the additional terms from friction.

6. SIMULATION RESULTS

In this section, we examine the zero-input responses of x_m and θ of all models in Fig. 3, where $x_m(0) = 0.1$, $\theta(0) = \pi/4$. The vibration of the response occurs due to the characteristic of the spring. However, it can be suppressed by the effect of the friction. Moreover, we notice that all models contain an integrator, so the zero-input responses does not necessarily converge to zero. Besides, the equilibrium state of (14) has multiple solutions as shown in (15). Hence, although the same initial values are given, the responses might converge to different values due to the nonlinear dynamic. However, the ratio of x_m and θ at the equilibrium is approximately equal to r which is corresponding to (15).

Subsequently, we apply the pulse input and obtain the simulated responses in Fig. 4. Once the input is applied to this system, the motor drives the belt in motion. After the input dies down, the motion stops at a certain point. In the case of linear model, the motion stops at the farthest position and demonstrates more ripples than those of the nonlinear and linearized models. The friction in the linearized model directly additively affects the damping term and the spring constant. Therefore, the motion of linearized model stops more quickly than that of the nonlinear model.

7. CONCLUSIONS

Three models of the servo-driven conveyor system were developed in this work. First, we derived the nonlinear dynamical model which incorporates the nonlinear spring and the friction model. In addition, the linearized model was obtained by the first-order approximation of the nonlinear model around the equilibrium points. When neglecting all nonlinearities, we obtained the simple linear model. The zero-input and zero-state responses of three models were compared in the simulation results. The linear model has the rapid responses because of neglecting the nonlinearities and has pure imaginary eigenvalues. Since the linearized model includes the damping term taken from the friction, it is corresponding to the real system better than the linear model. However, the linearized model ignores internal dynamics of the friction at low velocity. Thus, the added term to the spring stiffness, which corresponds to the break-away force, greatly affects the decay rate of the motion. Therefore, the nonlinear model is more precisely matched to the real system, but it increases the model complexity and requires the information of the friction dynamics. The future work is to find the suitable parameters for the model validation and explore the model which will be used for the controller design.

ACKNOWLEDGEMENTS

This work is part of the collaborative research under JICA project for AUN/SEED-Net whose sponsorship is greatly appreciated. The authors would like to acknowledge Ms. Tanipporn Rujiraapa and Mr. Paradorn Tiraprasert for the assistance of the hardware development.

REFERENCES

[1] M. E. Wroe and J. A. De Abreu-Garcia, "Analysis and Control of a Double Conveyor System With a Take-up Loop", *in 20th Int. Conf. on Industrial Electronics, Control and Instrumentation*, vol. 3, 1994, pp. 2023-2026.

[2] H. Takeuchi and Kang-Zhi Liu, "Velocity control of a mine truck system using rationally scaled $\mathcal{H}_\infty$ control", *in Proc. of the 35th IEEE Decision and Control*, vol. 1, 1996, pp. 767-772.

[3] T. Jeinsch, M. Sader, R. Noack, K. Barber, S. X. Ding, P. Zang, and M. Zhong, "A robust model-based information system for monitoring and fault detection of large scale belt conveyor systems", *in Proc. of the 4th World Congress on Intelligent Control and Automation*, vol. 4, 2002, pp. 3283-3287.

[4] E. Suhir, "Shock Protection with a Nonlinear Spring", *IEEE Trans. on Components, packaging, and Manufacturing Tech.*, vol. 18, no. 2, 1995, pp. 430-437.

[5] C. Canudas de Wit, H. Olsson, K. J. Åström, and P. Lischinsky, "A New Model for Control of Systems with Friction", *IEEE Trans. Aut. Control.*, vol. 40, no. 3, 1995, pp. 419-425.

[6] R. Kelly, Jeśus Llamas, and R. Campa, "A Measurement Procedure for Viscous and Coulomb Friction", *IEEE Trans. on Instrumentation and Measurement.*, vol. 49, no. 4, 2000, pp. 857-861.

[7] B. C. Kuo, *Automatic Control Systems*, Prentice Hall, 1995.

[8] R. H. A. Hensen, M. J.G. van de Molengraft, and M. Steinbuch, "Frequency Domain Identification of Dynamic Friction Model Parameters", *IEEE Trans. Control Sys. Tech.*, vol. 10, no. 2, 2002, 191-195.

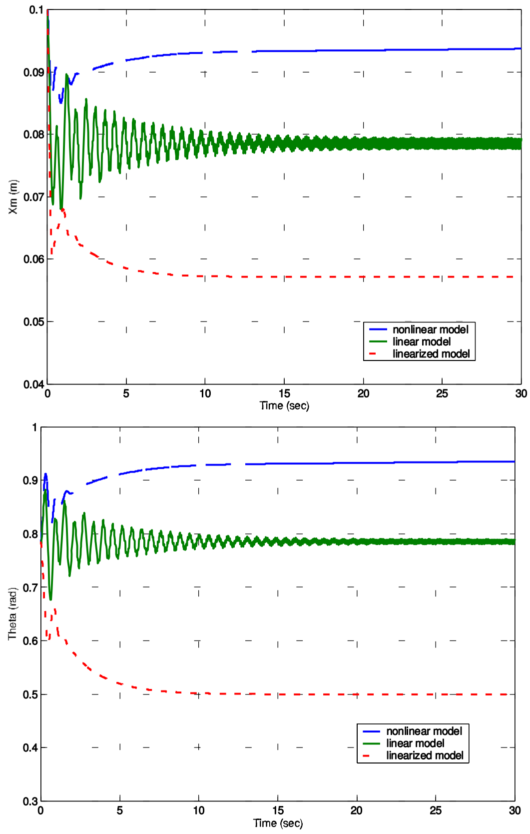

Fig. 3. The zero-input response of x_m and θ

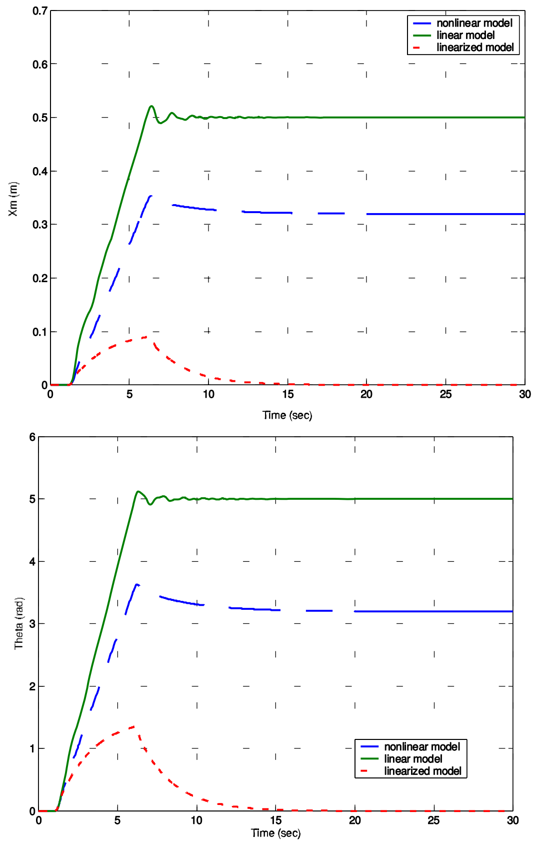

Fig. 4. The impulse response of x_m and θ